

# Preparation of liposomal amiodarone and investigation of its cardiomyocyte-targeting ability in cardiac radiofrequency ablation rat model

Ying Zhuge<sup>1,\*</sup>  
Zhi-Feng Zheng<sup>1,\*</sup>  
Mu-Qing Xie<sup>2</sup>  
Lin Li<sup>2</sup>  
Fang Wang<sup>1</sup>  
Feng Gao<sup>2,3</sup>

<sup>1</sup>Department of Cardiology, Shanghai First People's Hospital of Nanjing Medical University, <sup>2</sup>Department of Pharmaceutics, School of Pharmacy, <sup>3</sup>Shanghai Key Laboratory of Functional Materials Chemistry, East China University of Science and Technology, Shanghai, People's Republic of China

\*These authors contributed equally to this work

**Abstract:** The objective of this study was to develop an amiodarone hydrochloride (ADHC)-loaded liposome (ADHC-L) formulation and investigate its potential for cardiomyocyte targeting after cardiac radiofrequency ablation (CA) in vivo. The ADHC-L was prepared by thin-film method combined with ultrasonication and extrusion. The preparation process was optimized by Box–Behnken design with encapsulation efficiency as the main evaluation index. The optimum formulation was quantitatively obtained with a diameter of  $99.9 \pm 0.4$  nm, a zeta potential of  $35.1 \pm 10.9$  mV, and an encapsulation efficiency of  $99.5\% \pm 13.3\%$ . Transmission electron microscopy showed that the liposomes were spherical particles with integrated bilayers and well dispersed with high colloidal stability. Pharmacokinetic studies were investigated in rats after intravenous administration, which revealed that compared with free ADHC treatment, ADHC-L treatment showed a 5.1-fold increase in the area under the plasma drug concentration–time curve over a period of 24 hours ( $AUC_{0-24h}$ ) and an 8.5-fold increase in mean residence time, suggesting that ADHC-L could facilitate drug release in a more stable and sustained manner while increasing the circulation time of ADHC, especially in the blood. Biodistribution studies of ADHC-L demonstrated that ADHC concentration in the heart was 4.1 times higher after ADHC-L treatment in CA rat model compared with ADHC-L sham-operated treatment at 20 minutes postinjection. Fluorescence imaging studies further proved that the heart-targeting ability of ADHC-L was mainly due to the CA in rats. These results strongly support that ADHC-L could be exploited as a potential heart-targeting drug delivery system with enhanced bioavailability and reduced side effects for arrhythmia treatment after CA.

**Keywords:** liposomes, cardiomyocyte targeting, amiodarone hydrochloride, cardiac radiofrequency ablation

## Introduction

Cardiac radiofrequency ablation (CA) is a method usually used in the treatment of cardiac arrhythmias. During the operation, catheters are guided into the left atrium and used to create radiofrequency inflammatory lesions in the myocardial tissue in order to interrupt the aberrant electrical signals causing the arrhythmia.<sup>1</sup> Although the technique of CA has improved over the years, the occurrence of the side effect of atrial fibrillation after CA treatment has remained a serious problem. It is widely accepted that utilization of class I or class III antiarrhythmic drugs after CA operation could decrease the incidence of atrial fibrillation. Among these antiarrhythmic drugs, amiodarone hydrochloride (ADHC) is widely used to enhance the efficiency and reduce the side effects in CA operation for patients with cardiac arrhythmia.

Correspondence: Fang Wang  
Department of Cardiology, Shanghai First People's Hospital of Nanjing Medical University, 100 Haining Road, Hongkou District, Shanghai 200080, People's Republic of China  
Tel +86 21 6324 0090  
Email 1838750550@qq.com



ADHC is a highly effective drug in the treatment of various supraventricular and ventricular arrhythmias.<sup>2</sup> Nevertheless, side effects of ADHC have been observed due to its long half-life and the nonspecific accumulation in several nontarget tissues, especially in the thyroid. Its preferred accumulation in thyroid may lead to hypothyroidism or hyperthyroidism.<sup>3</sup> It has been reported that ADHC might precipitate out upon dilution, which may enhance the risk of blood vessel occlusion after intravenous injections.<sup>4</sup> Other side effects include cardiac toxicity, pulmonary toxicity, and liver dysfunction, which might also occur after long-term administration.<sup>5</sup> In addition, high doses of ADHC administration could cause hypotension and noncardiac death.<sup>6</sup> These drawbacks have greatly impeded long-term administration of ADHC. Therefore, novel delivery systems are greatly demanded for ADHC to enhance its therapeutic antiarrhythmic effects while reducing the severe side effects associated with it.

Liposomes have been widely used in construction of drug delivery systems. They are biodegradable and less toxic.<sup>7-9</sup> Typical liposomes are nanoscale spheres surrounded by lipid bilayers. The unique structure enables them to incorporate hydrophobic molecules such as ADHC within lipid bilayer walls.<sup>6,10</sup> Liposomal formulations are adjustable to improve drug solubility and stability, enhance their bioavailability, modify tissue distribution profiles of drugs, and target specific organs in cancer or inflammatory diseases.<sup>11-13</sup> Takahama et al<sup>6</sup> investigated the effects of liposomal amiodarone on lethal arrhythmias and hemodynamic parameters in an ischemia/reperfusion rat model. They discovered that the liposomal amiodarone targeting ischemic/reperfused myocardium could reduce the mortality due to lethal arrhythmia and the negative hemodynamic changes caused by amiodarone. Besides, more beneficial effects have been reported by other research groups, including enhanced cellular permeability of inflammatory lesions and disrupted vascular endothelial integrity.<sup>14,15</sup> All groups suggested that liposomes might be a promising heart-targeting drug delivery system for post-CA treatment. In this study, we prepared ADHC-loaded liposomes (ADHC-L) by thin-film method combined with ultrasonication and extrusion. The physicochemical characteristics of the nanoparticles, such as particle size, size distribution, and encapsulation efficiency (EE), were determined. The preparation processes were optimized by Box–Behnken design with EE as the determination index. The pharmacokinetic parameters of ADHC-L were investigated in rats. The tissue distribution of ADHC-L and fluorescence imaging of the heart after CA were also studied *ex vivo*.

## Materials and methods

### Chemicals and reagents

ADHC was purchased from Titanchem Co. Ltd (Shanghai, People's Republic of China). IR-775 chloride was purchased from Sigma-Aldrich Co. (St Louis, MO, USA). Cholesterol was purchased from Sinopharm Chemical Reagent Co. Ltd (Shanghai, People's Republic of China). Phosphatidylcholine (PC) was purchased from Lipoid GmbH Co. Ltd (Ludwigshafen am Rhein, Germany). Male Sprague Dawley rats were purchased from Cavens Biotechnology Co. Ltd (Nanjing, People's Republic of China). All other reagents used in this study were of high-performance liquid chromatography (HPLC) or reagent grade.

### Preparation of ADHC-L

ADHC-L was prepared by a modified procedure of film hydration method with sonication and extrusion to obtain small and uniform liposomes. PC, cholesterol, and ADHC were dissolved in 20 mL chloroform and poured into a round bottom flask. The solution was evaporated to dryness in a 60°C water bath by reduced pressure rotary evaporation. The formed dried film was then hydrated with deionized water. Small unilamellar liposomes were generated by sonication. Crude suspension was filtered through 0.45 µm Millipore membrane filters to remove the free ADHC crystals.

### Physicochemical and morphological characterization of ADHC-L

The particle size and surface zeta potential of the liposomes were analyzed by dynamic light scattering (NanoZS4700 nanoseries; Malvern Instruments, Malvern, UK). The samples were diluted with deionized water prior to determination. Mean size and polydispersity index were obtained from 70 times measurements. The morphology of ADHC-L was studied by transmission electron microscope (JASCO, Tokyo, Japan), and the samples were negatively stained with 1% phosphotungstic acid.

### EE determination

Concentration of the encapsulated ADHC was measured by HPLC (1260 series; Agilent Technologies, Santa Clara, CA, USA) analysis on a Platisil ODS-C18 column (4.6×250 mm, 5 µm; Dikma, Beijing, People's Republic of China). ADHC-L was diluted in methanol before measurement. The mobile phase consisted of 2% triethylamine solution (adjusted to pH 4.0 with phosphoric acid):methanol (13:87, v/v), which was delivered at an isocratic flow rate of 1.2 mL/min at 40°C. Ultraviolet light at 242 nm was used

for detection. The injection volume was 20  $\mu$ L. The EE was calculated using Equation 1:

$$EE (\%) = \frac{\text{Amount of ADHC in liposomes}}{\text{Total amount of ADHC}} \times 100 \quad (1)$$

## Optimization of ADHC-L preparation conditions by Box–Behnken design

Box–Behnken design was employed to optimize the preparation process of liposomes.<sup>16</sup> Three parameters (the weight ratio of PC to cholesterol, A; the weight ratio of PC to ADHC, B; ultrasonic time, C) which had significant effects on EE were selected, and EE was selected as the determination index. Three levels were chosen for each factor. These three factors at three levels were as follows: the weight ratio of PC to cholesterol (2:1, 6:1, and 10:1), the weight ratio of PC to ADHC (10:1, 30:1, and 50:1), and ultrasonic time (10, 20, and 30 minutes). A design matrix comprising 15 experimental runs was constructed. The nonlinear computer-generated quadratic model is given as Equation 2:

$$Y = b_0 + b_1A + b_2B + b_3C + b_{12}AB + b_{23}BC + b_{13}AC + b_{11}A^2 + b_{22}B^2 + b_{33}C^2 \quad (2)$$

in which Y was the determination value of index,  $b_0$  was the intercept,  $b_1$ – $b_{33}$  were regression coefficients, and A, B, and C were the factors investigated. The relationship between each factor and the index was fitted using data processing software Design-Expert trial Version 8.05 (Stat-Ease Inc., Minneapolis, MN, USA), and the following regression coefficients and constants were calculated. In addition, accuracy of the regression formula obtained was evaluated by fitness and correlation coefficient. Response surfaces which exhibited the relationship between each factor and the index were drawn according to the fitting equation. Finally, we selected the optimization formula from response surface drawing to prepare ADHC-L. In addition, verification experiments were carried out according to the optimization formula, and EE was tested in order to see whether the experimental results were consistent with the model.

## Pharmacokinetics of ADHC-L

For all in vivo experiments, male Sprague Dawley rats (270–300 g body weight) purchased from Nanjing Cavens Biotechnology Co. Ltd. were used. All animal experiments were carried out in accordance with the guidelines evaluated and approved by the ethics committee of East China University of Science and Technology. Animals were

given unlimited access to food and water and were kept in a 12 hour light-dark cycle.

A total of 12 rats were randomly divided into three groups: group A, free ADHC (3 mg/kg); group B, free ADHC (9 mg/kg); and group C, ADHC-L (3 mg ADHC/kg). The free ADHC and the ADHC-L were diluted in physiological saline up to 0.45 mL and immediately injected into the tail veins of rats. At 3, 10, 30, 60, 120, 240, 480, 720 and 1,440 minutes following intravenous injection, a blood sample (0.5 mL) was collected from the veins of fundus oculi. The samples were centrifuged at 8,000 rpm for 10 minutes to obtain plasma (0.1 mL). The plasma sample was mixed with 20  $\mu$ L of an internal standard solution of 100  $\mu$ g/mL durabolin. Then, 1.5 mL of acetonitrile was added to the plasma and mixed for 5 minutes. The mixture was centrifuged at 11,000 rpm for 5 minutes and the supernatant was transferred and dried under nitrogen.

The concentration of ADHC in the blood plasma was assessed by HPLC. The dried residue was mixed with 0.4 mL of methanol, and then 20  $\mu$ L of the sample was injected into the chromatograph. The mobile phase was 2% triethylamine solution (adjusted to pH 4.0 with phosphoric acid):methanol (18:82, v/v), which was delivered at an isocratic flow rate of 1.0 mL/min at 40°C. A reversed-phase Platisil ODS-C18 column (4.6 $\times$ 250 mm, 5  $\mu$ m; Dikma) was employed. Ultraviolet light at 242 nm was used for detection. The retention time of ADHC and durabolin was 8.4 and 9.2 minutes, respectively. Concentration data were dose-normalized and plotted as drug concentration–time curves in blood plasma. The area under the concentration–time curve (AUC) was calculated by the trapezoidal rule.

## Biodistribution of ADHC-L after CA

A total of 16 rats were randomly divided into four groups: group A, intravenous administration of free ADHC (3 mg/kg) after CA; group B, intravenous administration of ADHC-L (3 mg ADHC/kg) after CA; group C, intravenous administration of free ADHC (3 mg/kg) after thoracotomy without CA, which is also called sham-operated (SO) group; and group D, intravenous administration of ADHC-L (3 mg ADHC/kg) after SO. The free ADHC and the ADHC-L were diluted in physiological saline up to 0.45 mL. After basal anesthesia by intraperitoneal injection of urethane, the rats were intubated and the artificial respiration was applied to keep rats breathing.

A left thoracotomy was conducted in the fourth intercostal space of the rats to expose the heart. A clamp which was utilized to suspend the heart was also used as an indifferent electrode. Four radiofrequency lesions in a line per

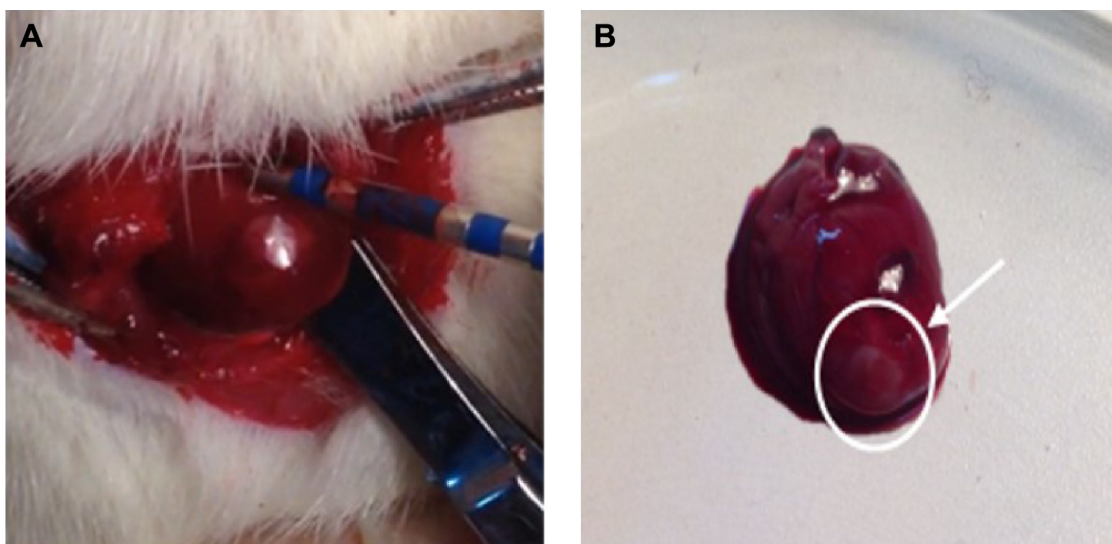


**Figure 1** The cardiac radiofrequency ablation of rats in situ and the inflammatory lesions of heart.

**Notes:** (A) Picture showing left ventricle ablation and (B) the heart of the rat after cardiac radiofrequency ablation. The white circle and the arrow denote radiofrequency ablation area.

rat were then performed on the free wall of the left ventricle with a customized catheter which had an electrode located at its tip (Figure 1A). Unipolar radiofrequency current with constant 12 W power for 15 seconds was created using a commercially available conventional radiofrequency generator (IBI-1500T8, Irvine Biomedical, Irvine, CA, USA). During each application, impedance was monitored. After the ablation, the white and circular lesions with defined margins were easily seen by visual inspection (Figure 1B). Then, the heart was immediately returned back to the thorax, and suture was used to close the chest.<sup>17,18</sup>

At 20 minutes following intravenous injection, the rats were killed. The principal organ samples (including heart, liver, spleen, lung, and kidney) were harvested, weighed, minced, and extracted in absolute methanol. The concentration of ADHC in the organ samples was assessed by HPLC described in previous section. Concentration data were dose-normalized. The results of biodistribution were expressed as the amount of ADHC uptake per gram of organ ( $\mu\text{g/g}$ ).

## Fluorescence imaging of the heart after CA

Fluorescence imaging of the heart was used to evaluate the heart-targeting ability of the prepared liposomes after CA. Fluorescence-labeled liposomes were prepared using IR-775, a near-infrared fluorescent dye ( $\lambda_{\text{excitation (em)}}$  = 770 nm and  $\lambda_{\text{emission (em)}}$  = 830 nm) with a low aqueous solubility (5.25  $\mu\text{g/mL}$ , 25°C), as the model drug. PC (405.0 mg), cholesterol (54.7 mg), ADHC (10.0 mg), and IR-775 (2.0 mg) were dissolved in 10 mL chloroform and poured into a round bottom

flask. The solution was evaporated to dryness in a 60°C water bath by reduced pressure rotary evaporation. The formed dried film was then hydrated with deionized water. Small unilamellar liposomes were generated by sonication for 30 minutes. Crude suspension was filtered through 0.45  $\mu\text{m}$  Millipore membrane filters to remove the free IR-775 crystals.

Rats were randomly divided into three groups: group A, intravenous administration of IR-775 loaded liposomes after SO; group B, intravenous administration of IR-775 loaded liposomes after CA; and group C, intravenous administration of physiological saline after CA. The CA was conducted as described above. At 20 minutes following intravenous injection, the rats were killed. The hearts were harvested, rinsed with phosphate-buffered saline, and the fluorescent images as well as the X-ray images were taken using the Kodak In-vivo Multispectral Imaging system (Kodak, NY, USA).

## Statistical analysis

Multiple group comparison was conducted by one-way analysis of variance with least significant difference using statistical software (SPSS Inc., Chicago, IL, USA). All data are presented as a mean value with standard deviation indicated (mean  $\pm$  standard deviation). *P*-values < 0.05 were considered to be statistically significant.

## Results and discussion

### Optimization of ADHC-L preparation conditions by Box–Behnken design

Response surface methodology (RSM) is a combined mathematical and statistical technique which is useful for planning

experiments, determining complex quantitative relationships between parameters and their responses, and identifying response optimizing factor combination.<sup>19,20</sup> The main advantage of RSM is to reduce the required experimental times, which could be less than would be needed in a full factorial design. It has already been widely applied to optimize formulation design in pharmaceutical studies.<sup>21</sup> Box–Behnken design is one of the commonly used RSM designs. When the number of factors is three, the experimental time could be reduced to the minimum.<sup>22</sup> It is widely acknowledged as one of the best statistical and analytical models.<sup>23</sup>

According to Box–Behnken designs, 15 preparation conditions and results are listed in Table 1. Analysis of variance for the experimental results and quadratic model are shown in Table 2, in which the small *P*-value for the model (<0.05) implied the model was significant. It indicated that the equation for EE was right and this method was reliable. The *P*-value for the “lack-of-fit” test was 0.5226 (>0.05), indicating that the quadratic model was adequate. The regression equation is as follows:

$$Y = 93.49 + 5.49A + 0.54B + 1.17C + 0.99AB + 1.33AC + 0.21BC + 5.91A^2 + 7.05B^2 + 1.34C^2 \quad (3)$$

The above regression equation quantitatively describes the effects of three independent variables on the index and their correlation. The adjusted *R*<sup>2</sup> for the predictive model was 0.7648, and the “Adeq Precision” of 7.534 revealed that the experimental results adequately fitted the equation selected.

To understand the predicted model better, three-dimensional graphs were mapped by plotting the response

**Table 1** Experimental values of objective variables

A (the weight ratio of PC to cholesterol)	B (the weight ratio of PC to ADHC)	C (ultrasonic time, min)	EE (%)
2	10	20	76.8
10	30	10	94.1
10	10	20	87.0
6	30	20	94.7
10	30	30	93.5
6	30	20	89.9
2	30	10	81.7
6	30	20	95.9
6	50	30	91.4
6	10	10	83.8
2	50	20	72.1
2	30	30	86.4
10	50	20	86.3
6	10	30	86.9
6	50	10	89.1

**Abbreviations:** ADHC, amiodarone hydrochloride; EE, entrapment efficiency; PC, phosphatidylcholine.

**Table 2** Statistical analysis of variance for the experimental results

Source	Sum of squares	df	Mean square	F value	P-value	Prob > F
Model	575.11	9	63.90	6.06	0.0307	Significant
A	241.45	1	241.45	22.89	0.0049	
B	2.33	1	2.33	0.22	0.6579	
C	10.88	1	10.88	1.03	0.3563	
AB	3.88	1	3.88	0.37	0.5706	
AC	7.05	1	7.05	0.67	0.4508	
BC	0.18	1	0.18	0.018	0.8998	
A*A	128.87	1	128.87	12.22	0.0174	
B*B	183.28	1	183.28	17.38	0.0087	
C*C	6.60	1	6.60	0.63	0.4647	
Residual	52.73	5	10.55			
Lack of fit	32.21	3	10.74	1.05	0.5226	Not significant
Pure error	20.52	2	10.26			
Cor total	627.84	14				

**Notes:** A, the weight ratio of PC to cholesterol; B, the weight ratio of PC to ADHC; C, ultrasonic time.

**Abbreviations:** df, degrees of freedom; cor, correlation; ADHC, amiodarone hydrochloride; PC, phosphatidylcholine.

versus two of the factors, while the third factor was fixed at its central level (Figure 2). As shown in Figure 2A, with increase in the weight ratio of PC to cholesterol, EE showed an initial increasing and later decreasing curve. Similar trend was observed as the weight ratio of PC to ADHC increased. Figure 2B demonstrates that with an increase in the weight ratio of PC to cholesterol, EE ascended at first and descended at last, just as shown in Figure 2A, while EE slowly increased as the ultrasonic time rose. Finally, Figure 2C also shows EE experienced a convex curvature with an increasing weight ratio of PC to ADHC. It can be predicted that with an increase in the weight ratio of PC to cholesterol, there is more space in the lipid bilayer to encapsulate ADHC; however, when the weight ratio increased to a certain value, the liquidity of lipid bilayer increased, causing instability of liposomes.

The optimum formulation was selected based on the criteria of obtaining the maximum value of EE. On the basis of the regression equation and the response surface models, the optimum formulation of liposomes was defined: the weight ratio of PC to cholesterol was 7.43, the weight ratio of PC to ADHC was 40.48, and the ultrasonic time was 30 minutes. Under this condition, the predictive maximum EE value was 96.75% and the actually measured value was 99.49%±13.31%. It could be seen that the actually measured value was quite close to the predictive value.

## Physicochemical and morphological characterization of ADHC-L

Particle size and zeta potential are the two most important parameters in liposome quality evaluation. In this study, we demonstrated that liposomal amiodarone was successfully

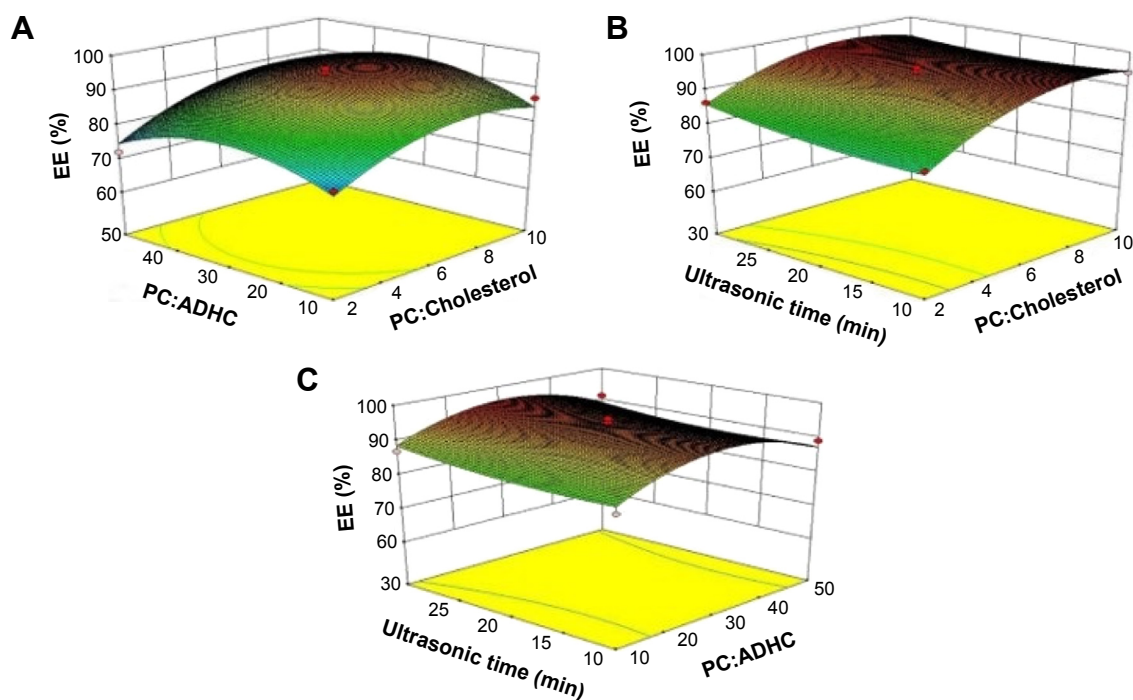


**Figure 2** Contour plots and three-dimensional response surfaces showing the effects of (A) the weight ratio of PC to cholesterol, (B) the weight ratio of PC to ADHC, and (C) ultrasonic time on the response of EE.

**Abbreviations:** ADHC, amiodarone hydrochloride; EE, entrapment efficiency; PC, phosphatidylcholine.

prepared using the film hydration method with sonication and extrusion. Under the optimum conditions, we obtained stabilized liposomes with a diameter of  $99.90 \pm 0.36$  nm, a polydispersity index of  $0.22 \pm 0.01$ , and a zeta potential of  $35.07 \pm 10.86$  mV, which were suitable for intravenous injection.

The morphology of ADHC-L was studied by transmission electron microscopy and the result is shown in Figure 3. All the liposomes were well-dispersed spherical particles with integrated bilayers.

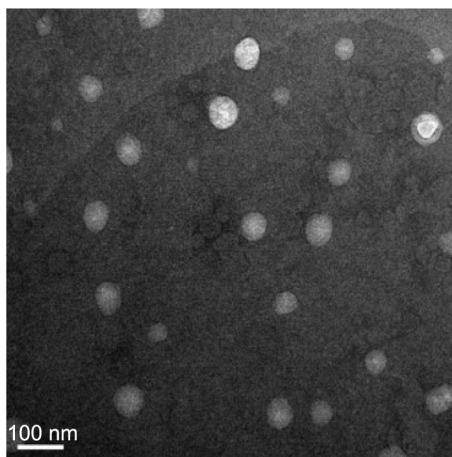


**Figure 3** Transmission electron microscopy photograph of amiodarone hydrochloride-loaded liposome.

## Pharmacokinetics of ADHC-L

The blood plasma level of ADHC concentration was determined at various time points after intravenous injection of a single dose of free ADHC (3 or 9 mg/kg) and ADHC-L (3 mg ADHC/kg). At the indicated time point, blood plasma level of ADHC was determined using HPLC.

As shown in Figure 4, the maximum plasma concentration of ADHC after the intravenous administration of free ADHC (3 or 9 mg/kg) and ADHC-L was reached at 3 minutes postinjection, and then a biphasic profile with a rapid initial

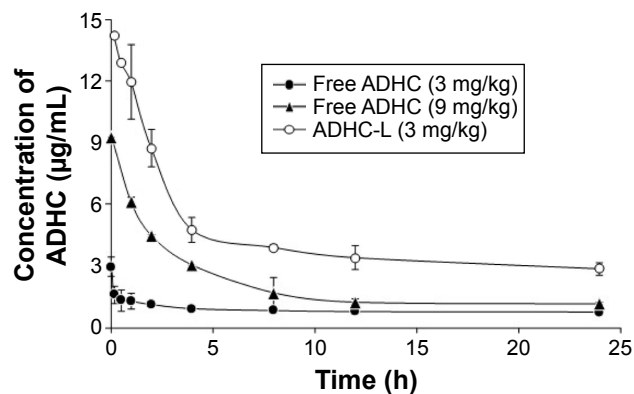


**Figure 4** Plasma concentration-time profiles of ADHC after a single intravenous injection of free ADHC (solid circles, 3 mg ADHC/kg or solid triangles, 9 mg ADHC/kg) and ADHC-L (empty circles, equivalent 3 mg ADHC/kg) in rats.

**Abbreviations:** ADHC, amiodarone hydrochloride; ADHC-L, amiodarone hydrochloride-loaded liposome.

drug elimination phase, followed by a slower elimination phase was observed. The rapid initial elimination phase was likely due to the reversible distribution between the central compartment and the peripheral compartments. Subsequently, a slower and irreversible elimination phase from the central compartment occurred by hepatic biotransformation or by renal excretion. The rapid initial elimination phase for 3 mg/kg free ADHC treatment was 10 minutes, while that for 9 mg/kg free ADHC treatment increased to 60 minutes. For ADHC-L treatment, the relative rapid elimination phase further increased to 240 minutes. In the extended postinjection period up to 24 hours, the ADHC plasma concentration in the rats treated with ADHC-L was 3.8-fold and 2.5-fold higher than that in the rats treated with 3 mg/kg free ADHC and 9 mg/kg free ADHC, respectively.

The pharmacokinetic parameters of free ADHC (3 or 9 mg/kg) and ADHC-L in rats after intravenous administration are shown in Table 3. The parameters like  $t_{1/2\beta}$  and mean residence time (MRT) of 3 mg/kg free ADHC and 9 mg/kg free ADHC treatment almost had no significant difference. Compared with 3 mg/kg free ADHC treatment, the  $AUC_{0-24h}$  (the area under the plasma drug concentration–time curve over a period of 24 hours) of 9 mg/kg free ADHC treatment increased by 2.6-fold due to the increment of administration dose. However, ADHC-L treatment showed a drastic increase in the half-life of the elimination phase  $t_{1/2\beta}$  (195.44 hours) compared with free ADHC administered at the same dose (28.71 hours), while the clearance rate of 3 mg/kg free ADHC treatment (0.07 L/h/kg) and 9 mg/kg free ADHC treatment (0.13 L/h/kg) was 3.5-fold and 6.0-fold that of ADHC-L treatment (0.02 L/h/kg), respectively. This suggests that the clearance rate of ADHC in the blood plasma decreased

significantly when ADHC was incorporated into liposomes. Moreover, ADHC-L treatment showed a 5.1-fold increase in  $AUC_{0-24h}$  and an 8.5-fold increase in MRT compared with 3 mg/kg free ADHC treatment, suggesting that ADHC-L caused the drug payload to be released in a more stable and sustained manner. The significant decrease in  $V_{ss}$  of ADHC-L treatment also demonstrates that a higher concentration of ADHC was retained in the blood, compared with that of free ADHC treatment. To sum up, when ADHC was incorporated into liposomes, both solubility and stability of ADHC improved. The liposomes could not only prevent ADHC from binding to plasma protein and increased the drug circulation time, particularly in the blood, but also significantly reduce the required ADHC dosage in treatment and, hence, decrease the dose-dependent toxicity.

## Biodistribution of ADHC-L after CA

To examine the biodistribution of ADHC-L and free ADHC after CA or SO, each formulation at a dose of 3 mg ADHC/kg was injected through the tail veins after the operation and the concentration of ADHC in principal organs was measured 20 minutes postinjection.

At 20 minutes postinjection (Figure 5), the heart uptake of ADHC was in the following order: ADHC-L CA > ADHC CA = ADHC-L SO > ADHC SO. ADHC-L CA treatment increased the heart uptake by fourfold compared with ADHC CA treatment. In addition, the concentration of ADHC in the heart of ADHC-L SO treatment was 1.8 times higher than that of ADHC SO treatment, suggesting that the liposome-based ADHC delivery could slightly increase drug targeting to the heart. However, the ADHC concentration in the heart of ADHC-L CA treatment was 4.1 times higher than that of ADHC-L SO treatment, indicating that the enhanced heart-targeting ability of ADHC-L was

**Table 3** Pharmacokinetic parameters of ADHC after a single dosage administration to rats

Pharmacokinetic parameters	Free ADHC (3 mg/kg)	Free ADHC (9 mg/kg)	ADHC-L (3 mg/kg)
$t_{1/2\alpha}$ (h)	0.08±0.04	1.33±0.18**	1.86±0.24**
$t_{1/2\beta}$ (h)	28.71±6.04	26.14±10.61	195.44±36.62**
$K_{el}$ ( $h^{-1}$ )	0.09±0.01	0.12±0.10*	0.09±0.01
CL (L/h/kg)	0.07±0.02	0.13±0.01*	0.02±0.01*
$V_{ss}$ (L/kg)	0.80±0.18	1.08±0.05	0.20±0.01*
MRT (h)	32.06±4.47	32.10±13.02	273.97±58.00**
$AUC_{0-24h}$ (mg·h/L)	20.69±1.10	52.91±0.37***	106.22±1.60***
$AUC_{0-\infty}$ (mg·h/L)	42.00±12.49	67.29±1.18	163.80±24.03**

**Notes:** Given values are mean ± SD (n=4). \* $P$ <0.05, \*\* $P$ <0.01, \*\*\* $P$ <0.001 versus free ADHC (3 mg/kg) treatment.

**Abbreviations:** ADHC, amiodarone hydrochloride; ADHC-L, amiodarone hydrochloride-loaded liposome; AUC, area under the concentration–time curve; CL, clearance;  $K_{el}$ , elimination rate constant; MRT, mean residence time; SD, standard deviation;  $t_{1/2\alpha}$ , half-life of distribution phase;  $t_{1/2\beta}$ , half-life of elimination phase;  $V_{ss}$ , steady-state distribution volume.

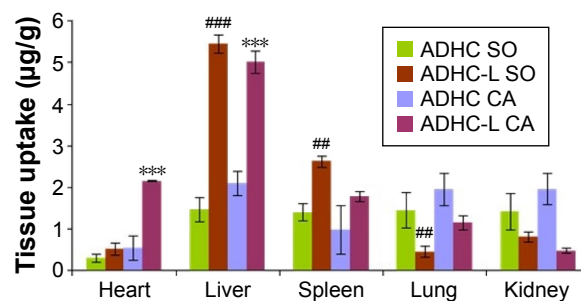


**Figure 5** Plots of ADHC biodistribution in rats 20 minutes after intravenous administration of free ADHC or ADHC-L at a dose of 3 mg ADHC/kg.

**Notes:** Given values are mean ± SD (n=4). \*\*\* $P$ <0.001 versus ADHC CA treatment. ### $P$ <0.01, #### $P$ <0.001 versus ADHC SO treatment.

**Abbreviations:** ADHC, amiodarone hydrochloride; ADHC-L, amiodarone hydrochloride-loaded liposome; CA, cardiac radiofrequency ablation; SO, sham-operated.

closely associated with CA, likely caused by the enhanced vascular leakage in the heart tissues with inflammatory lesions after CA treatment. It is known that CA could cause inflammatory lesions in the heart which are characterized by enhanced vascular leakiness. The “enhanced permeability and retention” effect will lead to selective accumulation of liposomes in tissues with inflammatory lesions compared with healthy tissues.<sup>24</sup>

Moreover, ADHC concentrations in the liver and spleen of ADHC-L CA and ADHC-L SO treatment increased significantly compared with those of free ADHC treatment, likely due to the favored passive targeting of liposomes to these mononuclear macrophage-rich organs. In contrast, the ADHC concentrations decreased in lung and kidney after ADHC-L CA and ADHC-L SO treatment. The latter phenomenon indicates that administration of ADHC-L could reduce the toxicity of ADHC.

## Fluorescence imaging of the heart after CA

Fluorescence imaging of the heart was used to evaluate the heart-targeting ability of the prepared liposomes after CA. The fluorescence-labeled liposomes were injected intravenously after CA or SO. Twenty minutes postinjection, the fluorescence imaging of rats’ heart were detected by the Kodak In-vivo Multi-spectral Imaging system.

As could be seen from Figure 6, the fluorescent signal of IR-775 after CA treatment was much stronger than that of SO treatment. The result further proved that the heart-targeting ability of ADHC-L was mainly associated with the CA.

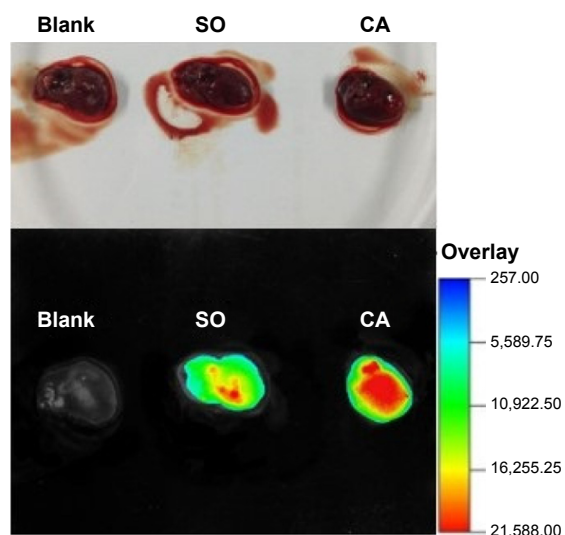


**Figure 6** Fluorescence imaging of rats’ hearts 20 minutes after intravenous administration of IR-775 loaded liposomes.

**Abbreviations:** CA, cardiac radiofrequency ablation; SO, sham-operated.

## Conclusion

In this study, a novel ADHC-L formulation with potential cardiomyocyte-targeting properties was successfully developed and its potential usage for heart-targeting after CA was investigated *ex vivo*. ADHC-L was prepared by modified thin-film method combined with ultrasonication and extrusion, and the preparation process was further optimized by Box–Behnken design. The optimum formulation led to liposomes suitable for intravenous injection with a well-dispersed spherical shape, high colloidal stability, and high EE. In addition, pharmacokinetic studies revealed that ADHC-L treatment showed a 5.1-fold increase in  $AUC_{0-24\text{ h}}$  and an 8.5-fold increase in MRT compared with free ADHC treatment, suggesting that ADHC-L could facilitate drug release in a more stable and sustained manner while increasing the circulation time of ADHC, especially in the blood. Moreover, biodistribution studies of ADHC-L demonstrated that ADHC concentration in heart was 4.1 times higher after ADHC-L CA treatment compared with ADHC-L SO treatment at 20 minutes postinjection. Fluorescence imaging studies further proved that the heart-targeting ability of ADHC-L was mainly due to the CA. These results strongly support that ADHC-L could be explored as a potential heart-targeting drug delivery system with enhanced bioavailability and reduced side effects for arrhythmia treatment after CA.

## Acknowledgments

The authors acknowledge the financial support from the Open Project Program of Shanghai First People’s Hospital of Nanjing Medical University (SKLFMC2014C01). This work was supported by the Science and Technology Commission of Shanghai Municipality (STCSM, contract no 10dz2220500).

## Disclosure

The authors report no conflicts of interest in this work.

## References

1. Rettmann ME, Holmes DR 3rd, Breen JF, et al. Measurements of the left atrium and pulmonary veins for analysis of reverse structural remodeling following cardiac ablation therapy. *Comput Methods Programs Biomed.* 2015;118(2):198–206.
2. Marcus FI, Fontaine GH, Frank R, Grosogoeat Y. Clinical pharmacology and therapeutic applications of the antiarrhythmic agent amiodarone. *Am Heart J.* 1981;101(4):480–493.
3. Lamprecht A, Bouligand Y, Benoit JP. New lipid nanocapsules exhibit sustained release properties for amiodarone. *J Control Release.* 2002;84(1–2):59–68.
4. Ward GH, Yalkowsky SH. Studies in Phlebitis VI: Dilution-induced precipitation of amiodarone HCl. *J Parenteral Sci Technol.* 1993;47(4):161–165.



5. Singh BN, Nademanee K. Amiodarone and thyroid function: Clinical implications during antiarrhythmic therapy. *Am Heart J.* 1983;106(4 Pt 2): 857–869.
6. Takahama H, Shigematsu H, Asai T, et al. Liposomal amiodarone augments anti-arrhythmic effects and reduces hemodynamic adverse effects in an ischemia/reperfusion rat model. *Cardiovasc Drugs Ther.* 2013;27(2): 125–132.
7. Arias JL. Liposomes in drug delivery a patent review (2007 – present). *Expert Opin Ther Patent.* 2013;23(11):1399–1414.
8. Qian S, Li C, Zuo Z. Pharmacokinetics and disposition of various drug loaded liposomes. *Curr Drug Metab.* 2012;13(4):372–395.
9. Li J, Wang X, Zhang T, et al. A review on phospholipids and their main applications in drug delivery systems. *Asian J Pharm Sci.* 2014; 10:81–98.
10. Safinya CR, Ewert KK. Liposomes derived from molecular vases. *Nature.* 2012;489(7416):372–374.
11. Semalty A, Semalty M, Rawat BS, Singh D, Rawat MS. Pharmacosomes: the lipid-based new drug delivery system. *Expert Opin Drug Deliv.* 2009; 6(6):599–612.
12. Malam Y, Loizidou M, Seifalian AM. Liposomes and nanoparticles: nanosized vehicles for drug delivery in cancer. *Trends Pharmacol Sci.* 2009;30(11):592–599.
13. Whitehead KA, Langer R, Anderson DG. Knocking down barriers: advances in siRNA delivery. *Nat Rev Drug Discov.* 2009;8(2): 129–138.
14. Horwitz LD, Kaufman D, Keller MW, Kong Y. Time course of coronary endothelial healing after injury due to ischemia and reperfusion. *Circulation.* 1994;90(5):2439–2447.
15. Dauber IM, VanBenthuyzen KM, McMurtry IF, et al. Functional coronary microvascular injury evident as increased permeability due to brief ischemia and reperfusion. *Circ Res.* 1990;66(4):986–998.
16. Yang S, Chen J, Zhao D, Han D, Chen X. Comparative study on preparative methods of DC-Chol/DOPE liposomes and formulation optimization by determining encapsulation efficiency. *Int J Pharm.* 2012; 434(1–2):155–160.
17. Antonio EL, Dos Santos AA, Araujo SR, et al. Left ventricle radio-frequency ablation in the rat: a new model of heart failure due to myocardial infarction homogeneous in size and low in mortality. *J Card Fail.* 2009;15(6):540–548.
18. Dos Santos LF, Antonio E, Serra A, et al. Radiofrequency ablation does not induce apoptosis in the rat myocardium. *Pacing Clin Electrophysiol.* 2012;35(4):449–455.
19. Cai WR, Gu XH, Tang J. Extraction, purification, and characterization of the polysaccharides from *Opuntia milpa alta*. *Carbohydr Polym.* 2007;71(3):403–410.
20. Lee WC, Yusof S, Hamid NA, Baharin BS. Optimizing conditions for hot water extraction of banana juice using response surface methodology (RSM). *J Food Eng.* 2006;75(4):473–479.
21. Hatambeygi N, Abedi G, Talebi M. Method development and validation for optimised separation of salicylic, acetyl salicylic and ascorbic acid in pharmaceutical formulations by hydrophilic interaction chromatography and response surface methodology. *J Chromatogr A.* 2011; 1218(35):5995–6003.
22. Rahman Z, Zidan AS, Khan MA. Non-destructive methods of characterization of risperidone solid lipid nanoparticles. *Eur J Pharm Biopharm.* 2010;76(1):127–137.
23. Ghasemi E, Sillanpää M, Najafi NM. Headspace hollow fiber protected liquid-phase microextraction combined with gas chromatography-mass spectroscopy for speciation and determination of volatile organic compounds of selenium in environmental and biological samples. *J Chromatogr A.* 2011;1218(3):380–386.
24. Schifflers RM, Banciu M, Metselaar JM, Storm G. Therapeutic application of long-circulating liposomal glucocorticoids in auto-immune diseases and cancer. *J Liposome Res.* 2006;16(3):185–194.

### International Journal of Nanomedicine

## Publish your work in this journal

The International Journal of Nanomedicine is an international, peer-reviewed journal focusing on the application of nanotechnology in diagnostics, therapeutics, and drug delivery systems throughout the biomedical field. This journal is indexed on PubMed Central, MedLine, CAS, SciSearch®, Current Contents®/Clinical Medicine,

Submit your manuscript here: <http://www.dovepress.com/international-journal-of-nanomedicine-journal>

Dovepress

Journal Citation Reports/Science Edition, EMBase, Scopus and the Elsevier Bibliographic databases. The manuscript management system is completely online and includes a very quick and fair peer-review system, which is all easy to use. Visit <http://www.dovepress.com/testimonials.php> to read real quotes from published authors.